Barriers to Diffusion of Plasma Membrane Proteins Form Early During Guinea Pig Spermiogenesis

Ann E. Cowan,* Lina Nakhimovsky,* Diana G. Myles,# and Dennis E. Koppel*
*Department of Biochemistry, University of Connecticut Health Center, Farmington, Connecticut 06030, and #Section of Molecular and Cellular Biology, University of California at Davis, Davis, California 95616 USA

ABSTRACT The plasma membrane of the mature guinea pig sperm is segregated into at least four domains of different composition. Previous studies have shown that some proteins localized within these domains are free to diffuse laterally, suggesting that barriers to protein diffusion are responsible for maintaining the nonuniform distribution of at least some surface proteins in mature sperm. The different membrane domains appear sequentially during sperm morphogenesis in the testis and during later passage through the epididymis. To determine when diffusion barriers become functional during sperm development, we examined the diffusion of two proteins that are expressed on the cell surface of developing spermatids and become segregated to different plasma membrane domains during the course of spermiogenesis. Both proteins exhibited rapid lateral diffusion throughout spermiogenesis, even after they become localized to specific regions of the surface membrane. These results suggest that barriers to membrane diffusion form concomitantly with membrane domains during spermiogenesis.

INTRODUCTION

The formation of membrane domains of discrete protein and lipid composition is a fundamental aspect of differentiation in many cell types. In several cases, for example, epithelial cells (Dragsten et al., 1981; van Meer and Simons, 1986; reviewed in Gumbiner, 1987), photoreceptors (Poo and Cone, 1974; Leibman and Entine, 1974; Papermaster et al., 1985, reviewed in Gumbiner and Louvard, 1985), and neurons (Dotti et al., 1991; Kobayashi et al., 1992; de Hoop and Dotti, 1993; but see Futerman et al., 1993, for an alternative viewpoint), there is evidence that barriers to diffusion at domain boundaries are responsible at least in part for maintaining the asymmetrical distribution of membrane components.

The tight junction between adjacent epithelial cells is currently the most well-characterized site that contains a diffusion barrier between plasma membrane domains. Proteins localized to tight junctions include the transmembrane protein occulin, intracellular peripheral membrane proteins ZO-1 and ZO-2, the cell adhesion molecule cadherin, and proteins that associate with the underlying cytoskeleton (Citi, 1993; Furuse et al., 1993; Gumbiner, 1993; Jesaitis and Goodenough, 1994). How these components are structurally integrated to form a diffusion barrier, however, is not yet well understood. The structural organization of domain boundaries that function as diffusion barriers in other cells remains largely unknown.

The mammalian sperm cell provides a useful system for investigating the nature of barriers to protein diffusion. The plasma membrane of guinea pig sperm is a remarkable mosaic. Four distinct membrane domains have been identified on the cell surface, termed the posterior tail (PT)1, anterior tail (AT), posterior head (PH), and anterior head (AH) domains (Primakoff and Myles, 1983). By using fluorescence redistribution after photobleaching (FRAP) techniques, several proteins localized to specific domains of mammalian sperm have been shown to be free to diffuse within their domain, with diffusion coefficients (D) of (1–5) $\times 10^{-9}$ cm^2/s and 80–100% of the protein exhibiting lateral mobility (Myles et al., 1984; Koppel et al., 1986; Cowan et al., 1987; Nehme et al., 1993). Because these are among the highest D values measured for proteins in biological membranes, these results provide strong evidence that membrane protein localization in these cases is maintained by some property of the domain boundary that prevents proteins from diffusing into adjacent regions of the membrane, i.e., a diffusion barrier. Based on these findings, it has been proposed that each of the boundaries that demarcate membrane domains on the sperm surface contains a diffusion barrier (Myles et al., 1987; Bartles, 1995), and specializations of the membrane and underlying cytoskeleton that may represent sites of diffusion barriers align precisely with boundaries between membrane domains (Friend, 1989; Cesario and Bartles, 1994).

The development of cell surface domains during sperm morphogenesis is a complex process. By following the surface localization of several proteins during spermiogenesis, we have shown that three plasma membrane domains appear sequentially during guinea pig sperm development in the testis (Cowan and Myles, 1993; see Fig. 1) in concert with morphological changes of the developing spermatid. Plasma membrane proteins may be segregated to the posterior tail (PT domain), anterior tail (AT domain), or whole head (WH) domain of the plasma membrane when the sperm exits the testis. The WH domain becomes further segregated into the anterior head (AH) and posterior head

Received for publication 9 May 1995 and in final form 3 April 1997.
Address reprint requests to Dr. Ann E. Cowan, Department of Biochemistry, University of Connecticut Health Center, Farmington, CT 06030. Tel.: 203-679-1449; Fax: 203-679-3408; E-mail: acowan@panda.uchc.edu.

0006-3495/97/07/507/10 $2.00

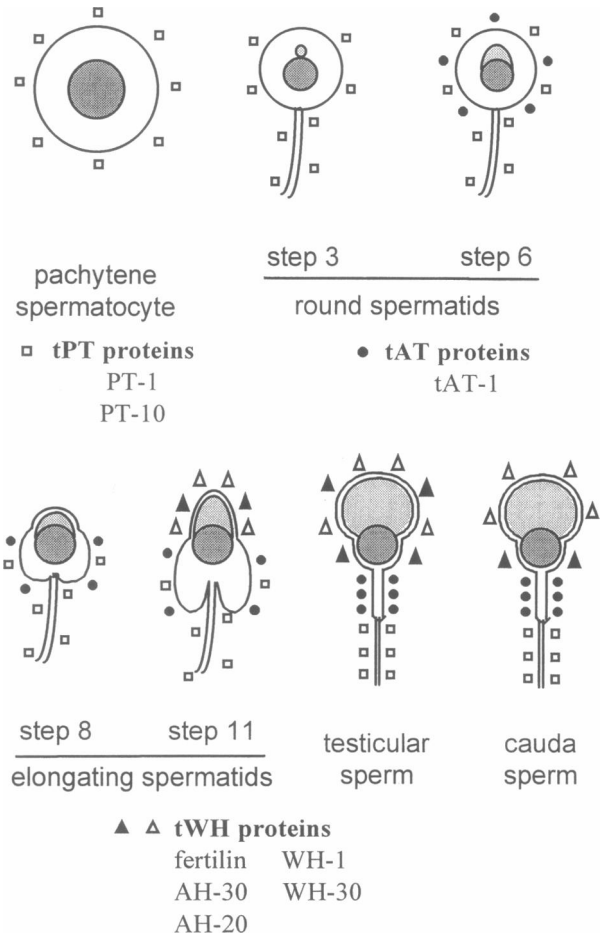

FIGURE 1 Summary of the surface localization of seven different plasma membrane proteins during spermatogenesis in the guinea pig. □, PT-1 and PT-10 proteins, which become localized to the posterior tail plasma membrane domain of testicular sperm (PT domain). ●, tAT-1 protein, which is restricted to the anterior tail plasma membrane domain of testicular sperm (AT domain). △, ▲, Five proteins restricted to the whole head domain of testicular sperm (WH domain). Some of these proteins will be further restricted to either the posterior head (PH) domain (▲) or anterior head (AH) domain (△) in sperm taken from the cauda epididymis. Steps refer to the 15 steps of spermiogenesis in the guinea pig (Leblond and Clermont, 1952). See text for details. (Reprinted from Carroll et al., 1995.)

(PH) domains as the sperm passes through the early regions of the epididymis (Phelps et al., 1990; G. Hunnicut et al., manuscript in preparation).

In the present study we have attempted to determine when diffusion barriers are formed during sperm development by examining the lateral diffusion of two proteins, PT-1 and tAT-1, that are progressively localized to the posterior tail and anterior tail, respectively, during spermiogenesis. Both proteins were found to exhibit rapid lateral diffusion at all stages of spermiogenesis, even after they became localized to specific domains. These results imply that barriers to diffusion at domain boundaries are formed as soon as the domains themselves are generated, and may be a prerequisite for the formation of membrane domains during spermiogenesis.

MATERIALS AND METHODS

Cells

Spermatogenic cells were isolated from Hartley male retired breeder guinea pigs (Elm Hill, Chelmsford, MA) by flushing the cells from slices of testis using a stream of Hanks' balanced salt solution lacking calcium (HBSS − Ca^{2+}) as previously described (Cowan and Myles, 1993). This mechanical method of cell isolation is relatively gentle and avoids the use of enzymes for cell dissociation. Measurements on testicular sperm were in some cases made on Percoll-purified sperm, using a modification of the method described by Cowan and Myles (1993). Briefly, a decapsulated testis was chopped into fine pieces in 10 ml HBSS − Ca^{2+}. The material was strained through a 100-μm nylon mesh, and the cell suspension was layered over 10 ml of 3% bovine serum albumin in HBSS − Ca^{2+} and centrifuged at 200 × g for 5 min. The cell pellet was resuspended in 5 ml HBSS − Ca^{2+}, and the cells were layered on a Percoll step gradient consisting of two steps of 90% and 40% Percoll prepared in HEPES-buffered saline. The cells were spun at 12,000 × g for 15 min, and the band of testicular sperm at the 90%–40% interface was recovered. The cells were diluted 10-fold in HBSS − Ca^{2+} and washed once to remove the Percoll.

Antibodies and cell staining

Immunofluorescence staining was done as described previously (Myles et al., 1981). PT-1 and tAT-1 proteins were stained using culture supernatants containing the PT-1 monoclonal antibody (mAb) (subclass IgG_{2b}) or the tAT-10 mAb (subclass IgG_{2a}; evidence that the tAT-10 mAb recognizes the tAT-1 protein is given in Results, Fig. 2), respectively, and a rhodamine-conjugated Fab fragment of goat anti-mouse IgG was prepared as described previously (Cowan and Myles, 1993). For some experiments, an Fab fragment of purified tAT-10 IgG, followed by the rhodamine-conjugated Fab fragment of goat anti-mouse IgG, was used. Incorporation of the lipid probe 1,1′-dihexadecyl-3,3,3′,3′-tetramethylindocarbocyanine perchlorate ($diIC_{16}$) (Molecular Probes, Eugene, OR) was done as described

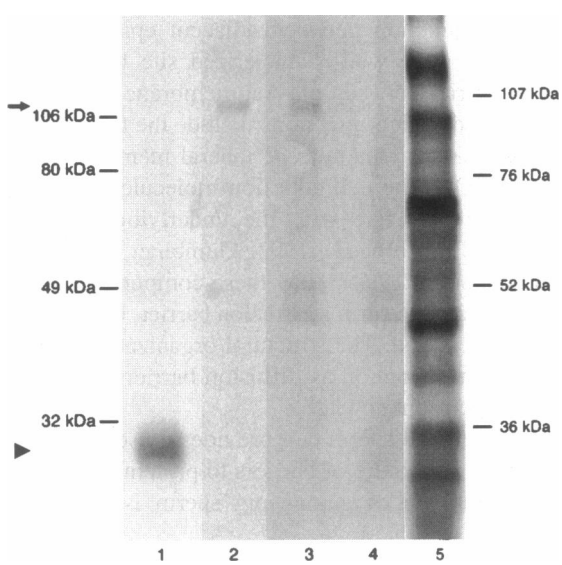

FIGURE 2 Identification of PT-1 and tAT-1 antigens by immunoprecipitation of biotinylated surface proteins. *Lane 1*, PT-1 mAb; *lane 2*, tAT-1 mAb; *lane 3*, tAT-10 mAb; *lane 4*, control mouse IgG; *lane 5*, total biotinylated proteins present in detergent extract from 10^5 cells. An arrowhead denotes the position of PT-1 protein; a small arrow denotes the position of the tAT-1 protein.

previously (Cowan et al., 1987), except that HBSS − Ca^{2+} was used as the cell medium.

Production of Fab fragment of tAT-10 IgG

tAT-10 IgG was purified from ascites fluid by using a protein A affinity column (Affigel; Pierce, Rockville, IL), following the manufacturer's instructions. The IgG was digested with papain coupled to agarose beads (Pierce), and the Fab fragment was purified as the eluate from a second protein A column.

Cell surface biotinylation and immunoprecipitation

Percoll-purified testicular sperm were suspended at 1×10^7/ml in HEPES-buffered saline (10 mM HEPES, pH 7.4, 0.15 M NaCl, and 2.7 mM KCl) and 600 μg sulfo-NHS biotin (Pierce) added from a freshly prepared stock solution at 100 mg/ml in dimethyl sulfoxide. After incubation for 30 min, the cells were layered on 5% Percoll and pelleted for 30 s in a microfuge. The cells were resuspended in 1% Triton X-100, 5 mM EDTA in Tris-buffered saline, pH 7.4, containing a protease inhibitor cocktail consisting of 1 μg/ml leupeptin, 1 mM phenylmethylsulfonyl fluoride, 2 μg/ml antipain, 10 μg/ml benzamidine, 1 μg/ml chymostatin, and 1 μg/ml pepstatin, and extracted for 30 min on ice. The extract was cleared of insoluble material by centrifugation at 100,000 × *g* for 1 h. Immunoprecipitations were done as previously described (Cowan and Myles, 1993), using extract from 10^6 cells per immunoprecipitation.

Fluorescence redistribution after photobleaching

The apparatus used for multipoint photobleaching measurements has been described previously (Koppel, 1979). We utilized a line photobleaching protocol, in which the laser beam is defocused along one axis to generate a focused line on the cell. The line photobleaching protocol reduces the analysis of diffusion to a one-dimensional problem. The line is sequentially positioned at 12 discrete points on the cell by using a galvanotropic mirror. A photomultiplier tube is used to obtain fluorescence intensity measurements at each of the 12 positions in a series of scans before and after the sample is bleached at one position with a high-intensity laser beam. For spermatocytes and round spermatids, the scan axis was randomly positioned on the cell; for elongating spermatids and sperm, the scan axis was generally at 90° to the anterior-posterior axis of the cell. The redistribution of fluorescence was analyzed by a new method based on analysis in Fourier space, as described below, using the software system MLAB (Civilized Software, Bethesda, MD).

The data were first analyzed in the spatial domain by using Gaussian fluorescence scans. This analysis allows one to extrapolate the data, theoretically, to long distances relative to the position of the bleach, which is necessary for the Fourier analysis that followed. This analysis follows the protocol described previously (Koppel, 1979; Nehme et al., 1993), except that it calibrated the prebleach scans with a nonlinear fit, to set up the postbleach scans with a second nonlinear fit, which contained a velocity drift. After analysis in the spatial domain, we fit the data with a new method of analysis based on Fourier transform space (Berk et al., 1993). The analyses in normal space and Fourier space are described in detail below.

The analysis in the spatial domain allows us to fit prebleach scans that show a combination of 1) an inhomogeneous intensity and 2) a slow drift that becomes apparent with the postbleach scans. We take this into account by first applying the Marquardt-Levenberg iterative curve-fitting algorithm (described in the MLAB reference manual; Civilized Software) to fit the prebleach scans to some function, like a six-parameter Fourier function, that fits the data. This Fourier function is then used as a multiplier in fitting the postbleach scans, with only the drift velocity as a single floating parameter to make the prebleach scans fit the rest of the normalized postbleach data. The Marquardt-Levenberg algorithm then fits the postbleach scans,

$$F_1(x_j, t_k) = F_0(x_j, t_k)[1 - f(x_j, t_k)] \quad (1)$$

where $F_0(x_j, t_k)$ is the Fourier transform of the prebleach data, with $f(x_j, t_k)$ taking the functional form of Koppel (1979) and Nehme et al. (1993),

$$f(x_j, t_k) = \frac{A}{(1 + 4Dt_k/w^2)^{1/(2d)}} \exp\left[- \frac{(x_j - x_0 + vt_k)^2/w^2}{(1 + 4Dt_k/w^2)} \right] + B \exp\left[- \frac{(x_j - x_0 + vt_k)^2}{w^2} \right] + C, \quad (2)$$

where v is the postbleach drift velocity, D is the diffusion coefficient, w is the width of the bleaching beam, C takes into account the possible offset of the bleaching beam by scattering, d is the dimensionality (1 equals one-dimensionality provided by the cylindrical lens) of the bleaching configuration, and the percentage recovery, $\%R$, equals $100 \times A/(A + B)$. The weights are computed dynamically during the fit. Before each iteration, the vector of weight functions is computed and used. We use the function

$$\sigma(x_j, t_k) = (vt_j + x_k < m\Delta x) \wedge (vt_k + x_j > \Delta x), \quad (3)$$

a logical AND function of two statements which ensure that the x value of each postbleach point falls within the range of the prebleach points before the drift occurs, where Δx is the space between points, and m is the number of points in a scan (= 12).

For the analysis in Fourier space, each postbleach scan $[f(x_j, t_k)]$ is extended in space by the theoretical form (Eq. 2). In this way, the Fourier transform of the whole scan is calculated as follows:

$$g(\mu_n, t_k) = \frac{|\Sigma_j f(x_j, t_k) \exp(-2\pi i \mu_n x_j)|}{\Sigma_j f(x_j, t_k)} \quad (4)$$

The Marquardt-Levenberg algorithm then fits the postbleach scans individually,

$$g(\mu_n, t_k) = a_n[\exp(-4\pi^2 \mu_n^2 D t_k) + b] \quad (5)$$

with $\%R = 100/(1 + b)$.

RESULTS

The PT-1 and tAT-1 proteins are progressively restricted to specific plasma membrane domains during spermiogenesis. In previous work, we have surveyed the surface localization of a number of plasma membrane proteins, including PT-1 and tAT-1, on spermatocytes and developing spermatids (Cowan and Myles, 1993). The results of this work are depicted in Fig. 1 to illustrate the plasma membrane localization of PT1 and tAT-1 in relation to other sperm plasma membrane proteins during development. The PT-1 protein (depicted as *open squares* in Fig. 1) is expressed on the surface of pachytene spermatocytes. After meiosis and elongation of the axoneme in step 1 of spermgenesis, the PT-1 protein is present in the flagellar plasma membrane, but is also still found on the entire cell surface of early round spermatids. The tAT-1 protein (depicted as *closed circles* in Fig. 1) can first be detected on the surface of live cells at the cap phase of development. When it first appears on the surface, tAT-1 protein is restricted to the plasma membrane of the cell body, and is not observed on the flagellar plasma

membrane. The appearance of tAT-1 in the plasma membrane of the cell body of cap-phase spermatids marks the earliest time that plasma membrane proteins have been shown to be restricted to a specific domain in guinea pig spermatids. When the spermatid begins to elongate, the PT and tAT proteins are absent from the plasma membrane that is closely apposed to the acrosome at the anterior surface of the cell. This region of the plasma membrane will become the WH domain. The tAT-1 protein is restricted to the lobe of cytoplasm that forms posterior to the nucleus, and the PT-1 protein is found in the membrane of the cytoplasmic lobe and the flagellum. Four proteins that will become localized to the WH domain (*open and filled triangles* in Fig. 1) do not appear on the cell surface until the maturation phase, when they are found in the plasma membrane over the acrosome, and in the cytoplasmic lobe plasma membrane. The final step in spermiogenesis is the removal of the cytoplasmic lobe as the residual body. This event, called spermiation, separates the sperm cell from its association with the seminiferous epithelium, and the sperm is released into the lumen of the seminiferous tubule. After this event, tAT-1 remains in the AT domain, PT-1 protein is present exclusively in the PT domain, and the WH proteins are restricted to the WH plasma membrane domain.

Identification of the PT-1 mAb and tAT-10 mAb antigens

The PT-1 antigen has previously been defined as a protein, based on its sensitivity to protease and sedimentation behavior on sucrose gradients (Myles et al., 1984), but a polypeptide has not yet been identified by immunoprecipitation or immunoblotting. The tAT-1 antigen was identified as a 115-kDa protein in immunoprecipitates of surface ^{125}I-labeled cells using the tAT-1 mAb (Cowan and Myles, 1993), which is an IgM and therefore is not useful for FRAP experiments. We used biotin to label surface proteins of testicular sperm and prepared detergent extracts for immunoprecipitation with the PT-1 mAb and the tAT-10 mAb, an IgG class mAb that exhibits immunofluorescence staining similar to that of the tAT-1 mAb. The PT-1 mAb immunoprecipitates a polypeptide of M_r 29,000 from detergent extracts of surface-biotinylated testicular sperm (Fig. 2, *lane 1*). The tAT-10 mAb immunoprecipitates a M_r 115,000 polypeptide from these extracts (Fig. 2, *lane 2*), which comigrates with the tAT-1 protein immunoprecipitated by the tAT-1 mAb (Fig. 2, *lane 3*). To demonstrate the specificity of the mAbs, total biotinylated proteins present in the detergent extract of testicular cells is shown in lane 5.

Because neither the PT-1 or tAT mAbs recognize denatured antigen in immunoblots, it has not been possible to establish whether these two proteins are integral to the plasma membrane or if they are peripheral membrane proteins associated with other integral membrane components. However, as demonstrated in the results of Cowan and Myles (1993, and see Discussion here), these two proteins are highly specific to a discrete membrane domain; if they themselves are not integral to the membrane, they must be bound to a localized membrane component.

Diffusion of the PT-1 protein during spermiogenesis

The lateral mobility of the PT-1 protein at different times during spermatogenesis was determined using fluorescence redistribution after photobleaching (FRAP). On spermatocytes and round spermatids, the PT-1 protein is found on the entire cell surface (see Fig. 1). The protein was found to diffuse rapidly both on spermatocytes [$D = (7.7 \pm 4.7) \times 10^{-10}$ cm^2/s; percentage recovery, $\%R = 81 \pm 12$] and on the cell body of round spermatids [$D = (7.1 \pm 3.7) \times 10^{-10}$ cm^2/s; $\%R = 78 \pm 11$; Table 1 and Fig. 3 *A*, *A'*, and *B*, *B'*]. When spermatid elongation begins at step 8 of spermiogenesis, the PT-1 protein becomes restricted to the plasma membrane of the flagellum and the cytoplasmic lobe that protrudes from the posterior region of the cell body. Both D and $\%R$ for the PT-1 protein measured on the cytoplasmic lobe of elongating spermatids remain essentially unchanged [$D = (9.8 \pm 4.6) \times 10^{-10}$ cm^2/s; $\%R = 78 \pm 11$, Table 1 and Fig. 3, *C*, *C'*], even though the distribution of the protein changes from a nonlocalized to a localized distribution.

After release of the developing spermatid from the seminiferous epithelium, the PT-1 protein is localized exclusively to the PT domain of the sperm that exits the testis. On testicular sperm, D for PT-1 protein in the PT domain was approximately twofold slower than on the cytoplasmic lobe plasma membrane of spermatids [$D = (3.3 \pm 1.5) \times 10^{-10}$ cm^2/s; Table 1 and Fig. 3 *D*, *D'*], although the percentage recovery was unchanged ($\%R = 78 \pm 14$). The value of D measured on testicular sperm is approximately sevenfold less than previously reported for PT-1 on cauda sperm ($D = 2.4 \times 10^{-9}$ cm^2/s; Myles et al., 1984). To verify that this

TABLE 1 Diffusion coefficients (D) and percentage recovery ($\%R$) for PT-1 protein at different stages of spermatogenesis

Stage of development	Localization of PT-1	Site of measurement	$D \times 10^{10}$ (cm^2/s)*	$\%R$*	n
Spermatocytes	Whole cell	Whole cell	7.7 ± 4.7	81 ± 12	14
Round spermatids	Whole cell	Cell body	7.1 ± 3.7	78 ± 11	20
Elongating spermatids	Cytoplasmic lobe and tail	Cytoplasmic lobe	9.8 ± 4.6	78 ± 11	22
Testicular sperm	Posterior tail	Posterior tail	3.3 ± 1.5	78 ± 14	19
Cauda sperm	Posterior tail	Posterior tail	15 ± 5	88 ± 12	7

*Mean ± SD.

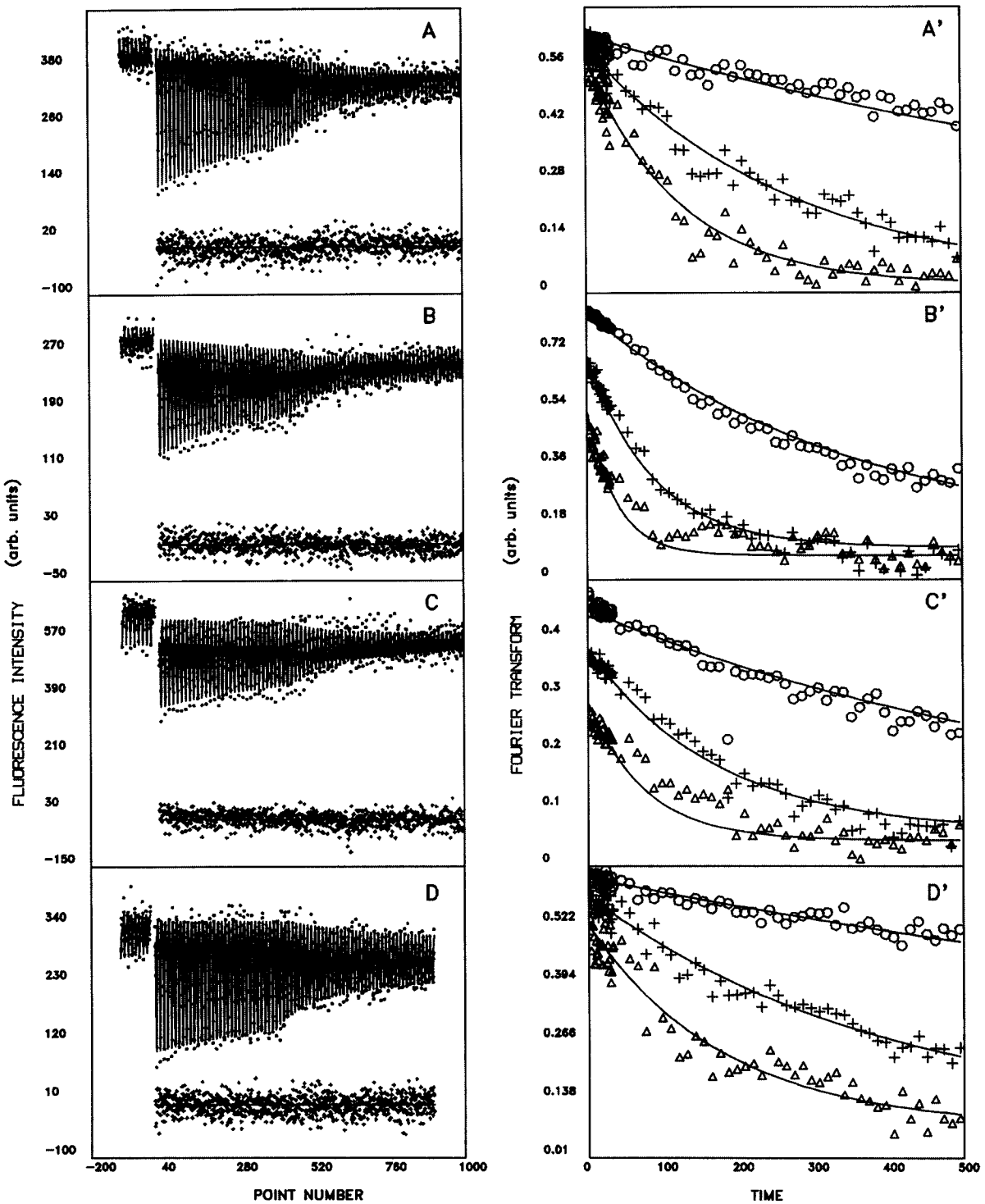

FIGURE 3 Diffusion of PT-1 during spermatogenesis. Data from representative photobleaching experiments show the redistribution of PT-1 protein in the plasma membrane of a pachytene spermatocyte (*A*, *A'*), the cell body of a round spermatid (*B*, *B'*), the residual cytoplasm of an elongating spermatid (*C*, *C'*), and the posterior tail of a testicular sperm (*D*, *D'*). (*A–D*) Fluorescence intensity (○) monitored at 12 discrete lines separated by 0.5 μm. In the middle of the experiment, the time between scans was increased by a factor of 11. The solid line shows the fit to Eq. 2 (see Materials and Methods). Crosses beneath the curves show the residuals from the fit. (*A'–D'*) Three lowest spatial frequencies of the Fourier transform of the data.

difference in D between testicular sperm and the previously reported value on cauda sperm does not reflect differences in the methods utilized, measurements were also made using cauda sperm, and results [$D = (1.5 \pm 0.5) \times 10^{-9}$; $\%R = 88 \pm 12$, Table 1] similar to those reported by Myles et al. (1984) were obtained.

Diffusion of the tAT-1 protein during spermiogenesis

When the tAT-1 protein is first detected in the plasma membrane, it is already localized; it is found on the cell body but not on the tail of round spermatids. FRAP measurements using the tAT-10 IgG to label round spermatids show that the tAT-1 protein diffuses laterally in the plasma membrane of the cell body at the earliest stages where measurements can be made [$D = (8.8 \pm 4.0) \times 10^{-10}$ cm^2/s; $\%R = 71 \pm 9$; Table 2 and Fig. 4 *A*, *A'*]. Similar results were obtained by using the Fab fragment of the tAT-10 IgG (data not shown), although the fluorescence intensity was substantially lower when the Fab fragment was used.

As the new WH domain emerges in elongating spermatids, the tAT-1 protein becomes restricted to the cytoplasmic lobe. Similar to the results obtained for the PT-1 protein, the tAT-1 protein continues to exhibit substantial lateral diffusion, even though it has become further restricted to the plasma membrane of the cytoplasmic lobe [$D = (8.2 \pm 4.9) \times 10^{-10}$ cm^2/s, $\%R = 69 \pm 15$; Table 2 and Fig. 4 *B*, *B'* and *C*, *C'*]. Even in early (step 8) elongating spermatids, we find no evidence for a transient immobilization of the protein on the cytoplasmic lobe as it initially becomes localized (Table 2 and Fig. 4 *C*, *C'*).

After the sperm is released from the seminiferous epithelium at spermiation, tAT-1 protein is restricted to the AT domain. The tAT-1 protein on testicular sperm is mobile, but exhibits a slower recovery than observed at earlier stages, with $D = (3.9 \pm 3.0) \times 10^{-10}$ cm^2/s and $\%R = 53 \pm 15$ (Table 2 and Fig. 4, *D*, *D'*) when measured using the using the Fab fragment of the tAT-10 IgG. When the intact tAT-10 IgG was used to label testicular sperm, the probe was found to be essentially immobile on the time scale of the FRAP experiments (data not shown).

Diffusion of the lipid probe diIC$_{16}$

We also examined the lateral mobility of a lipid probe, diIC$_{16}$, in spermatids and testicular sperm. We observed a threefold decrease in D for diIC$_{16}$ in the plasma membrane of testicular sperm ($D \approx 0.8 \times 10^{-8}$ cm^2/s; Table 3) compared to the cell body of round spermatids [$D = (2.5 \pm 1.9) \times 10^{-8}$ cm^2/s] or the cytoplasmic lobe of elongating spermatids [$D = (2.9 \pm 2.3) \times 10^{-8}$ cm^2/s]. No evidence for differences in lipid mobility in different regions of the testicular sperm plasma membrane was found. D for diIC$_{16}$ in testicular sperm was similar to previous measurements of D for diIC$_{14}$ in sperm retrieved from the cauda epididymis (Cowan et al., 1987). In testicular sperm, essentially complete recovery of fluorescence was observed ($\%R \approx 90$; Table 3). However, in spermatids the $\%R$ was somewhat lower ($\%R \approx 70$). We observed that some diIC$_{16}$ appeared to be internalized over time during the FRAP experiments using spermatids. It therefore seemed possible that the lower %R observed with spermatids might reflect internalization of diIC$_{16}$ by endocytosis in spermatids, but not in testicular sperm. When spermatids were maintained at 4°C after labeling with diIC$_{16}$ to reduce the rate of internalization, the $\%R$ increased to 88 ± 8%, whereas D was unchanged [$D = (1.6 \pm 0.8) \times 10^{-8}$ cm^2/s, $n = 11$].

DISCUSSION

Barriers to membrane protein diffusion are thought to be an important mechanism for maintaining the diversity of plasma membrane domains in the guinea pig sperm. By analyzing the diffusion of membrane proteins during spermatogenesis, we have found that localized proteins are free to diffuse in the plasma membrane at the earliest times that they exhibit a localized distribution. These results are consistent with the interpretation that diffusion barriers exist at domain boundaries when membrane domains can first be identified during development.

On mature sperm, localized membrane proteins exhibit lateral diffusion coefficients in the range of (1–5) $\times 10^{-9}$ cm^2/s (Myles et al., 1984; Koppel et al., 1986; Cowan et al., 1987; Nehme et al., 1993), with 80–100% of the protein diffusing. These values of D are among the highest observed for proteins in biological membranes, and thus indicate that barriers to lateral diffusion of membrane proteins exist at the domain boundaries. D values measured for tAT-1 and PT-1 on spermatids approach these values, but are slightly lower, in the range of (0.7–1.0) $\times 10^{-9}$ cm^2/s, with 70–90% recovery. Slower diffusion cannot, in itself, explain the maintenance of localized distributions of proteins in spermatids. For example, PT-1 would be expected to equilibrate into the head plasma membrane region of early elongating spermatids in 1.5–4 min (calculated as $d^2/2D \pm 1$ SD, assuming d, the diameter of the head region, is 5 μm).

The slight decrease in D does suggest, however, the existence of interactions that impede the lateral diffusion of

TABLE 2 Diffusion coefficients (*D*) and percentage recovery (%*R*) for tAT-1 protein at different stages of spermiogenesis

Stage of development	Localization of tAT-1	Site of measurement	$D \times 10^{10}$ (cm^2/s)*	%*R**	*n*
Round spermatids	Cell body	Cell body	8.8 ± 4.0	71 ± 9	10
Step 8 elongating spermatids	Cytoplasmic lobe	Cytoplasmic lobe	8.8 ± 3.3	79 ± 9	13
Steps 9–11 elongating spermatids	Cytoplasmic lobe	Cytoplasmic lobe	8.2 ± 4.9	69 ± 15	12
Testicular sperm	Anterior tail	Anterior tail	3.9 ± 3.0	53 ± 15	10

*Mean ± SD.

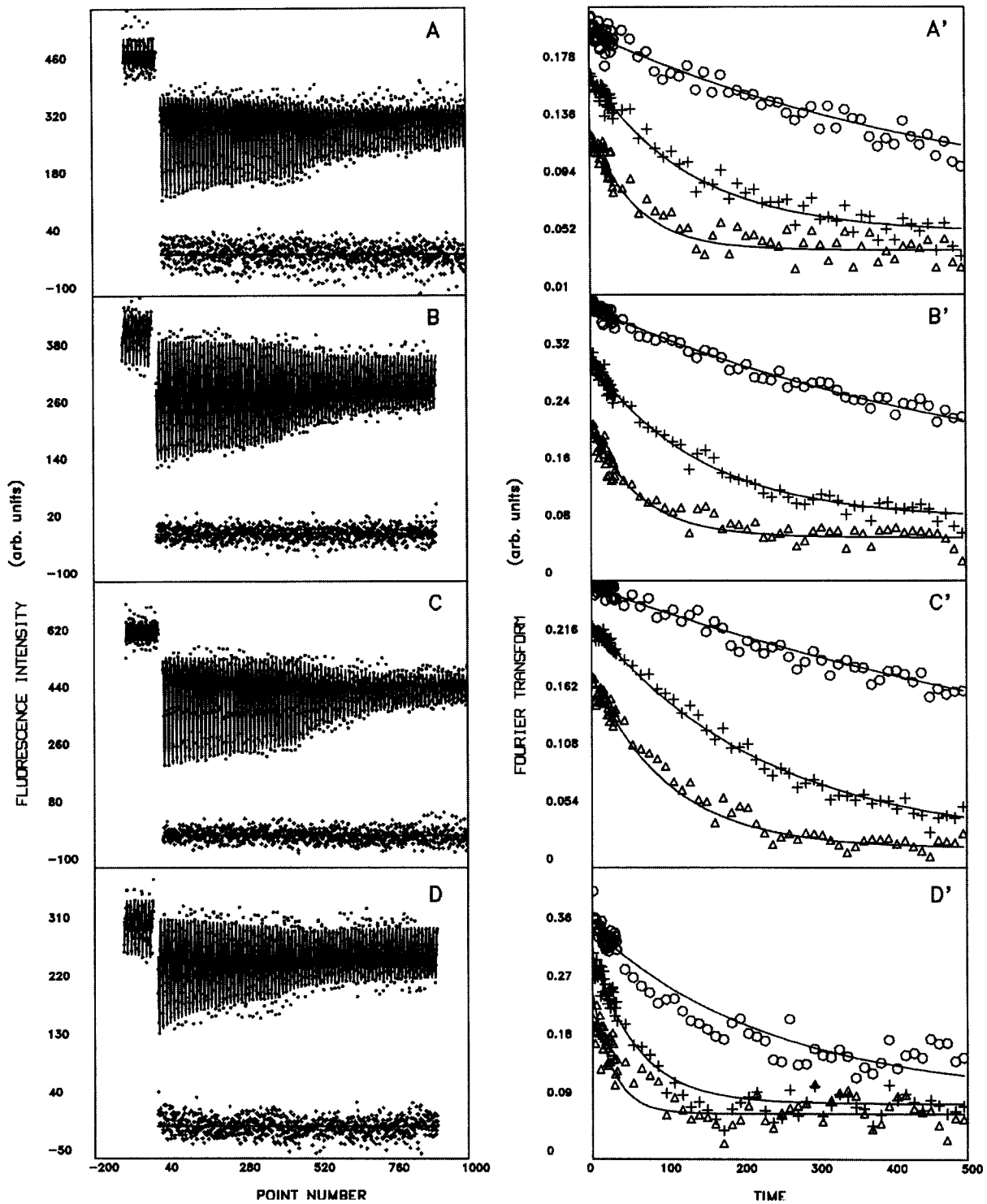

FIGURE 4 Diffusion of tAT-1 protein during spermiogenesis. Data from representative photobleaching experiments show the redistribution of tAT-1 protein in the plasma membrane of the cell body of round spermatids (*A*, *A'*), the residual cytoplasm of early (step 8) elongating spermatids (*B*, *B'*), later (step 9–11) elongating spermatids (*C*, *C'*), and the anterior tail region of a testicular sperm (*D*, *D'*). The left and right panels are as described in the legend to Fig. 3.

tAT-1 and PT-1. Hypotheses accounting for the observation that many proteins exhibit less than theoretical "free" lateral diffusion coefficients include either transient binding interactions with immobilized elements, or transient diffusion barriers that result from a submembraneous or extracellular matrix (reviewed in Saxton, 1990). Could such interactions

TABLE 3 Diffusion coefficients (D) and percentage recovery (%R) for C_{16}dil at different stages of spermiogenesis

Stage of development	Site of measurement	$D \times 10^8$ (cm^2/s)*	%R*	n
Round spermatids	Cell body	2.5 ± 1.9	69 ± 14	18
Elongating spermatids	Cytoplasmic lobe	2.9 ± 2.3	71 ± 14	10
Testicular sperm	Anterior head	0.86 ± 0.34	96 ± 9	10
	Posterior head	0.76 ± 0.21	91 ± 7	13
	Anterior tail	0.89 ± 0.20	90 ± 8	10
	Posterior tail	0.99 ± 0.40	90 ± 7	12

*Mean ± SD.

reflect a localization mechanism other than a diffusion barrier? If immobilized binding elements were localized to a specific membrane domain, they could potentially serve to concentrate a membrane protein within that domain. Consider a cell with two membrane domains, one of which contains immobilized binding components for a given membrane protein. At equilibrium, some of the membrane protein is unbound and diffuses at the theoretical limit throughout both domains, whereas bound protein ($D = 0$) exists only in one domain. Assuming that the exchange of bound and free protein is fast relative to the measurement, the measured D reflects a time average of D for freely diffusing protein and for bound protein (see Koppel, 1981). From Koppel (1981) it can be shown that, when the exchange of bound and free is rapid compared to the diffusion measurement,

$$D_{(\text{free+bound})}C_{(\text{free+bound})} = C_{(\text{free})}D_{(\text{free})} + C_{(\text{bound})}D_{(\text{bound})} \quad (6)$$

and therefore,

$$\frac{D_{(\text{free+bound})}}{D_{(\text{free})}} = \frac{C_{(\text{free})}}{C_{(\text{free+bound})}} \quad (7)$$

where $C_{(\text{free})}$, $C_{(\text{free + bound})}$ represent the concentrations of protein, and $D_{(\text{free + bound})}$ is the apparent D of the protein as measured by FRAP.

According to this scenario, at equilibrium the concentration of free protein will be equal in the two domains, and the ratio $C_{(\text{free})}/C_{(\text{free + bound})}$ is the degree to which the protein is concentrated in one domain. For example, transient interactions in one domain that reduce D by a factor of 10 could conceivably result in a 10-fold concentration of the protein, assuming that all of the interactions that restrict diffusion are localized to one domain.

For PT-1 in elongating spermatids, $D_{(\text{free + bound})} = 9.8 \times 10^{-10}$ cm^2/s. If $D_{(\text{free})}$ is assumed to be 5×10^{-9} cm^2/s (the largest D measured for a protein in a biological membrane), the ratio of $D_{(\text{free + bound})}/D_{(\text{free})} = 0.2$. From Eq. 7, then, the protein could be concentrated by a factor of 5 in one domain by this mechanism. In confocal images of elongating spermatids stained with PT-1 mAb and Rh-Fab second antibody, fluorescence intensity associated with the plasma membrane of the cytoplasmic domain was, on average, 13-fold higher than fluorescence intensity in the whole-head domain (average of eight cells measured; unpublished results). Because the fluorescence associated with the whole-head domain could not be distinguished from background, this represents a lower limit for the degree of concentration of PT-1 protein in the PT domain. Similarly, D for tAT-1 on round spermatids was measured to be 8.8×10^{-9} cm^2/s, which would yield a maximum concentration effect of six-fold by the transient interaction hypothesis. Confocal images of elongating spermatids stained with tAT-1 mAb staining showed no fluorescence above background in the whole-head domain, whereas fluorescence associated with the cytoplasmic lobe plasma membrane was 13 times background levels (average of 10 cells; unpublished results). Thus, based on the measured D, it seems unlikely that localized transient interactions could account for the localized distributions of either PT-1 or tAT-1 on elongating spermatids. The most straightforward interpretation of the experimental results is that the barriers to diffusion at the domain boundaries are created early in spermiogenesis, when the membrane domains are first created.

The first indication that plasma membrane domains exist on guinea pig spermatids is the appearance of the tAT-1 protein on the cell body plasma membrane. Our results suggest that a diffusion barrier exists at the boundary between the flagellum and the cell body at this stage of development. This boundary is the developmental antecedent of the boundary between the posterior tail and anterior tail region (refer to Fig. 1), which in mature sperm is characterized by the annulus, a circumferential ring of integral membrane proteins associated with submembranous fibrous material (Fawcett et al., 1970; Friend and Fawcett, 1974). It has previously been proposed that the annulus represents a barrier to protein diffusion (Myles et al., 1987; Friend, 1989), and a precursor to the annulus is present at the junction between the flagellum and cell body in round spermatids (Fawcett et al., 1970; Baccetti et al., 1978). Thus the appearance of this structure correlates with the development of separate membrane domains and a barrier to diffusion.

A third plasma membrane domain, the tWH domain, can first be distinguished by the absence of the PT-1 and tAT-1 proteins from the plasma membrane overlying the developing acrosome at step 8. The finding that both the tAT-1 and PT-1 proteins diffuse rapidly in the membrane of the cytoplasmic lobe, even though they are restricted from entering the tWH domain, suggests that a barrier to diffusion also exists at the boundary between these domains. This boundary is the developmental antecedent of the head/tail junction

in mature sperm; in elongating spermatids it is characterized by a structure termed the nuclear ring (Fawcett et al., 1971; Rattner and Olson, 1973), which anchors a sheath of microtubules (the manchette) to the plasma membrane. During spermatid elongation, the nuclear ring migrates caudally to the head/tail junction. At present it is not clear how the structures present at this domain boundary in spermatids are developmentally related to the structure of the head/tail junction in the mature spermatozoon.

The PT-1 protein and the tAT-1 protein exhibited slower diffusion in their respective domains on testicular sperm. In addition, D for PT-1 in testicular sperm is 4.1-fold lower than D for cauda sperm measured here and 7.6-fold lower than cauda sperm as reported by Myles et al. (1984). Because only the intact IgG was available to examine PT-1 diffusion, the reduced D could result from increased cross-linking by the divalent probe on testicular sperm. For tAT-1 protein, however, a monovalent probe was used to measure diffusion of tAT-1 in testicular sperm; thus the lower D, in fact, reflects a decrease in the mobility of the protein. It is interesting that the GPI-anchored PH-20 protein, present in the entire plasma membrane of testicular sperm, exhibits highly restricted lateral mobility on testicular sperm (Phelps et al., 1988), whereas in cauda sperm, PH-20 exhibits relatively rapid diffusion (Cowan et al., 1987; Phelps et al., 1988). The lipid probe C_{16}diI also showed a threefold reduction in D in testicular sperm compared to spermatids. It may be that there is a general decrease in the mobility of surface molecules on testicular sperm. In light of the many changes in the sperm plasma membrane and extracellular matrix that occur during late stages of spermiogenesis and epididymal passage (Eddy, 1988), it is interesting and perhaps not surprising that relatively large differences in lateral mobility of different components are observed. Exactly how these changes in lateral mobility reflect differences in plasma membrane composition and structure remains to be elucidated, as does how changes in lateral mobility relate to changes in localization and the functional state of specific membrane proteins.

In other species of mammalian sperm, such as ram and mouse, lipid probes such as diC_{16} have been shown to exhibit regionalized differences in both D and $\%R$ in testicular and mature sperm (Wolf and Voglmayr, 1984; Wolf et al., 1986). These results suggested that differences in lipid miscibility in the different plasma membrane domains might be a factor in maintaining the distinct compositions of different regions of the sperm plasma membrane. However, we found no evidence for regionalized differences in D for diC_{16} in the testicular sperm plasma membrane in the guinea pig, nor did we observe evidence of an immobile fraction of the lipid probe.

Significant immobile fractions (10–30%) of PT-1 and tAT-1 were observed at all stages of testicular development. In the case of spermatocytes and spermatids, endocytosis may well have contributed to the immobile fractions, as was found to be the case for C_{16}diI. It is unlikely, however, that endocytosis is a significant factor in testicular sperm. It is also possible that some of the immobile fraction could result from trace amounts of divalent probe in the second antibody, although this same probe yields high percentage recoveries (88 $\pm$ 12%) in the case of PT-1 measured in cauda sperm.

The development of barriers to diffusion during sperm development is likely to play an integral role in the development of membrane domains. The question of how membrane proteins are delivered to the correct domain during sperm development has only recently been explored (reviewed in Bartles, 1995), and several different mechanisms for localization have been proposed. The GPI-anchored PH-20 protein in guinea pig initially appears over the entire surface of the sperm cell in round spermatids and remains unlocalized through the remainder of testicular development. During epididymal passage it becomes restricted to the posterior head domain by a mechanism that involves directed migration of the protein into the posterior head domain (Phelps et al., 1990). The simultaneous appearance of different proteins in different plasma membrane domains implies that an intracellular sorting mechanism, similar to that known to exist in epithelial cells, targets insertion of proteins to the correct membrane domain. Vectorial targeting has been proposed to account for both the appearance of the CE9 protein in rat (Cesario et al., 1995) and an isoform of angiotensin-converting enzyme in mouse and rat (Sibony et al., 1994) in the tail plasma membrane domain late in spermiogenesis, at about the same time that fertilin and other head proteins appear in the WH and cytoplasmic lobe membrane in guinea pig.

Based on the finding that proteins destined for different regions of the plasma membrane first appear on the sperm surface at different times in sperm development, Cowan and Myles (1993) (see Fig. 1) have speculated that targeting of some membrane proteins to the correct surface domain may, in part, rely on coordinating when specific proteins are inserted into the plasma membrane with the development of barriers to diffusion. This hypothesis suggests that a diffusion barrier is erected to generate a boundary, and the bulk of new plasma membrane components are then primarily directed to one side of the boundary. The result that diffusion barriers are likely to exist early in spermiogenesis is at least consistent with this model. It is necessary, however, to point out that the appearance of a protein in a restricted domain does not necessarily reflect targeted insertion, but could also result from random membrane insertion and rapid removal from inappropriate domains, by either transcytosis or degradation in inappropriate domains. Both transcytosis (Mostov et al., 1993) and domain-specific degradation (Wang et al., 1990) have been observed in epithelial cells, but it has not yet been possible to address whether these mechanisms occur in spermatids.

Clearly, additional studies are needed to identify what mechanisms are utilized to target plasma membrane components to specific domains in sperm. In addition, although the present results suggest that diffusion barriers exist when protein localization to specific domains can first be identi-

fied, they do not indicate whether barriers might be present at earlier times. Experiments to address this possibility are currently in progress. Finally, it is not at all clear what the nature of the diffusion barriers in sperm might be, and future work will be directed toward achieving a molecular understanding of the construction of diffusion barriers in sperm.

This work was supported by National Institues of Health grants GM 23585 (D.K.) and HD 16580 (D.M.).

REFERENCES

Baccetti, B., E. Bigliardi, and A. G. Burrini. 1978. The cell surface during mammalian spermiogenesis. *Dev. Biol.* 63:187–196.

Bartles, J. R. 1995. The spermatid plasma membrane comes of age. *Trends Cell Biol.* 5:400–404.

Berk, D. A., F. Yuan, M. Leunig, and R. K. Jaqin. 1993. Fluorescence photobleaching with spatial Fourier analysis: Measurement of diffusion in light-scattering medium. *Biophys. J.* 65:2428–2436.

Cesario, M. M., and J. R. Bartles. 1994. Compartmentalization, processing and redistribution of the plasma membrane protein CE9 on rodent spermatozoa. Relationship of the annulus to domain boundaries in the plasma membrane of the tail. *J. Cell Sci.* 107:561–570.

Cesario, M. M., K. Ensrud, D. W. Hamilton, and J. R. Bartles. 1995. Biogenesis of the posterior-tail plasma membrane domain of the mammalian spermatozoon: targeting and lateral redistribution of the posterior-tail domain-specific transmembrane protein CE9 during spermiogenesis. *Dev. Biol.* 169:473–486.

Citi, S. 1993. The molecular organization of tight junctions. *J. Cell Biol.* 121:485–489.

Cowan, A. E., and D. G. Myles. 1993. Biogenesis of surface domains during spermiogenesis in the guinea pig. *Dev. Biol.* 155:124–133.

Cowan, A. E., D. G. Myles, and D. E. Koppel. 1987. Lateral diffusion of the PH-20 protein on guinea pig sperm: evidence that barriers to diffusion maintain plasma membrane domains in mammalian sperm. *J. Cell Biol.* 104:917–923.

de Hoop, M. J., and C. G. Dotti. 1993. Membrane traffic in polarized neurons in culture. *J. Cell Sci.* 17(Suppl.):85–92.

Dotti, C. G., R. Parton, and K. Simons. 1991. Polarized sorting of glypiated proteins in hippocampal neurons. *Nature.* 349:158–161.

Dragsten, P. R., R. Blumenthal, and J. S. Handler. 1981. Membrane asymmetry in epithelia: is the tight junction a barrier to diffusion in the plasma membrane? *Nature.* 294:718–722.

Eddy, E. M. 1988. The spermatozoon. *In* The Physiology of Reproduction. E. Knobil and J. Neill, editors. Raven Press, New York. 27–68.

Fawcett, D. W., W. A. Anderson, and D. M. Phillips. 1971. Morphogenetic factors influencing the shape of the sperm head. *Dev. Biol.* 26:220–251.

Fawcett, D. W., E. M. Eddy, and D. M. Phillips. 1970. Observations on the fine structure and relationships of the chromatid body in mammalian spermatogenesis. *Biol. Reprod.* 2:129–153.

Friend, D. S. 1989. Sperm maturation: membrane domain boundaries. *Ann. N.Y. Acad. Sci.* 567:208–567.

Friend, D. S., and D. W. Fawcett. 1974. Membrane differentiations in freeze-fractured mammalian sperm. *J. Cell Biol.* 63:641–664.

Furuse, M., T. Hirase, M. Itoh, A. Nagafuchi, S. Yonemura, S. Tsukita, and S. Tsukita. 1993. Occludin: a novel integral membrane protein localizing at tight junctions. *J. Cell Biol.* 123:1777–1788.

Futerman, A. H., R. Khanin, and L. A. Segel. 1993. Lipid diffusion in neurons. *Nature.* 362:119.

Gumbiner, B. 1987. Structure, biochemistry, and assembly of tight junctions. *Am. J. Physiol.* 253:C749–C758.

Gumbiner, B. M. 1993. Breaking through the tight junction barrier. *J. Cell Biol.* 123:1631–1633.

Gumbiner, B., and D. Louvard. 1985. Localized barriers in the plasma membrane: a common way to form domains. *Trends Biochem. Sci.* 10:435–438.

Jesaitis, L. A., and D. A. Goodenough. 1994. Molecular characterization and tissue distribution of ZO-2, a tight junction protein homologous to ZO-1 and the Drosophila discs-large tumor suppressor protein. *J. Cell Biol.* 124:949–961.

Kobayashi, T., B. Storrie, K. Simons, and C. G. Dotti. 1992. A functional barrier to movement of lipids in polarized neurons. *Nature.* 359:647–650.

Koppel, D. E. 1979. Fluorescence redistribution after photobleaching: a new multipoint analysis of membrane translational dynamics. *Biophys. J.* 28:281–292.

Koppel, D. E. 1981. Association dynamics and lateral transport in biological membranes. *J. Supramol. Struct. Cell. Biochem.* 17:61–67.

Koppel, D. E., P. Primakoff, and D. G. Myles. 1986. Fluorescence photobleaching analysis of cell surface regionalization. *In* Applications of Fluorescence in the Biomedical Sciences. D. L. Taylor, A. S. Waggoner, F. Lanni, R. F. Murphy, and R. Birge, editors. Alan R. Liss, New York. 477–497.

Leblond, C. P., and Y. Clermont. 1952. Spermiogenesis of rat, mouse, hamster and guinea pig as revealed by the "periodic acid-fuchsin sulfurous acid" technique. *Am. J. Anat.* 90:167–200.

Leibman, P. A., and G. Entine. 1974. Lateral diffusion of visual pigment in photoreceptor disk membranes. *Science.* 185:457–458.

Mostov, K. E., and G. Apodaca, B. Aroeti, and C. Okamoto. 1993. Plasma membrane protein sorting in polarized epithelial cells. *J. Cell Biol.* 116:577–583.

Myles, D. G., D. E. Koppel, A. E. Cowan, B. M. Phelps, and P. Primakoff. 1987. Rearrangement of sperm surface antigens prior to fertilization. *Ann. N.Y. Acad. Sci.* 513:262–273.

Myles, D. G., P. Primakoff, and A. R. Bellvé. 1981. Surface domains of the guinea pig sperm defined by monoclonal antibodies. *Cell.* 23:433–439.

Myles, D. G., P. Primakoff, and D. E. Koppel. 1984. A localized surface protein of guinea pig sperm exhibits free diffusion in its domain. *J. Cell Biol.* 98:1905–1909.

Nehme, C. L., M. M. Cesario, D. G. Myles, D. E. Kopel, and J. R. Bartles. 1993. Breaching the diffusion barrier that compartmentalizes the transmembrane glycoprotein CE9 to the posterior tail plasma membrane domain of the rat spermatozoon. *J. Cell Biol.* 120:687–694.

Papermaster, D. S., B. G. Schneider, and J. C. Besharse. 1985. Vesicular transport of newly synthesized opsin from the Golgi apparatus toward the rod outer segment. *Invest. Ophthalmol. Visual Sci.* 26:1386–1404.

Phelps, B. M., D. E. Koppel, P. Primakoff, and D. G. Myles. 1990. Evidence that proteolysis of the surface is an initial step in the mechanism of formation of sperm cell surface domains. *J. Cell Biol.* 111: 1839–1847.

Phelps, B. M., P. Primakoff, D. E. Koppel, M. G. Low, and D. G. Myles. 1988. Restricted lateral diffusion of PH-20, a PI-anchored sperm membrane protein. *Science.* 240:1780–1782.

Poo, M.-m., and R. A. Cone. 1974. Lateral diffusion in the photoreceptor membrane. *Nature.* 247:438–441.

Primakoff, P., and D. G. Myles. 1983. A map of the guinea pig sperm surface constructed with monoclonal antibodies. *Dev. Biol.* 98:417–428.

Rattner, J. B., and G. Olson. 1973. Observations on the fine structure of the nuclear ring of the mammalian spermatid. *J. Ultrastruct. Res.* 43: 438–444.

Saxton, M. J. 1990. The membrane skeleton of erythrocytes: models of its effect on lateral diffusion. *Int. J. Biochem.* 22:801–809.

Sibony, M., D. Segretain, and J.-M. Gasc. 1994. Angiotensin-converting enzyme in murine testis: step-specific expression of the germinal isoform during spermiogenesis. *Biol. Reprod.* 50:1015–1026.

van Meer, G., and K. Simons. 1986. The function of tight junctions in maintaining differences in lipid composition between the apical and the basolateral cell surface domains of MDCK cells. *EMBO J.* 5:1455–1464.

Wang, A. Z., G. K. Ojakian, and W. J. Nelson. 1990. Steps in the morphogenesis of a polarized epithelium. I. Uncoupling the roles of cell-cell and cell-substratum contact in establishing plasma membrane polarity in multicellular epithelial (MDCK) cysts. *J. Cell Sci.* 95:153–165

Wolf, D. E., S. S. Hagopian, and S. Ishijima. 1986. Changes in sperm plasma membrane lipid diffusibility after hyperactivation during in vitro capacitation in the mouse. *J. Cell Biol.* 102:1372–1377.

Wolf, D. E., and J. K. Voglmayr. 1984. Diffusion and regionalization in membranes of maturing ram spermatozoa. *J. Cell Biol.* 98:1678–1684.